Published in final edited form as:
Dev Biol. 2009 April 15; 328(2): 493–505. doi:10.1016/j.ydbio.2009.02.014.

Enamel-free teeth: *Tbx1* deletion affects amelogenesis in rodent incisors

Javier Catón[a], **Hans-Ulrich Luder**[b], **Maria Zoupa**[a], **Matthew Bradman**[a], **Gilles Bluteau**[b], **Abigail S. Tucker**[a], **Ophir Klein**[c,d], and **Thimios A. Mitsiadis**[b,*]

[a]Department of Craniofacial Development, King's College London, GKT Dental Institute, London SE1 9RT, UK [b]Department of Orofacial Development and Structure, Institute of Oral Biology, ZZMK, Faculty of Medicine, University of Zurich, Plattenstrasse 11, CH-8032 Zurich, Switzerland [c]Departments of Orofacial Sciences and Pediatrics, University of California at San Francisco, San Francisco, CA, 94143, USA [d]Institute of Human Genetics, University of California at San Francisco, San Francisco, CA, 94143, USA

Abstract

TBX1 is a principal candidate gene for DiGeorge syndrome, a developmental anomaly that affects the heart, thymus, parathyroid, face, and teeth. A mouse model carrying a deletion in a functional region of the *Tbx1* gene has been extensively used to study anomalies related to this syndrome. We have used the *Tbx1* null mouse to understand the tooth phenotype reported in patients afflicted by DiGeorge syndrome. Because of the early lethality of the *Tbx1*−/− mice, we used long-term culture techniques that allow the unharmed growth of incisors until their full maturity. All cultured incisors of *Tbx1*−/− mice were hypoplastic and lacked enamel, while thorough histological examinations demonstrated the complete absence of ameloblasts. The absence of enamel is preceded by a decrease in proliferation of the ameloblast precursor cells and a reduction in *amelogenin* gene expression. The cervical loop area of the incisor, which contains the niche for the epithelial stem cells, was either severely reduced or completely missing in mutant incisors. In contrast, ectopic expression of *Tbx1* was observed in incisors from mice with upregulated Fibroblast Growth Factor signalling and was closely linked to ectopic enamel formation and deposition in these incisors. These results demonstrate that *Tbx1* is essential for the maintenance of ameloblast progenitor cells in rodent incisors and that its deletion results in the absence of enamel formation.

Keywords

T-box genes; Tbx1; Transcription factors; Sprouty genes; Amelogenin; FGF; Incisor; Ameloblast; Enamel; Amelogenesis; Tooth development; Mouse; Epithelial stem cells

Introduction

DiGeorge syndrome (DGS) or velocardiofacial syndrome, also known as 22q11 deletion syndrome (22q11DS), is a common haploinsufficiency developmental disorder affecting approximately 1 in 4000 live births. The great majority of DGS cases result from de novo mutations, but this syndrome can also be inherited in an autosomal dominant fashion. Patients with DGS display a variety of clinical manifestations including abnormalities of the cardiac

*Corresponding author. Fax: +41 446343310. thimios.mitsiadis@zzmk.uzh.ch. .

outflow tract and aortic arch, thymus aplasia or hypoplasia, hypoparathyroidism, learning and/or behavioral disorders, and a range of malformations within the craniofacial region that includes an abnormal face, mandibular retrognathia and cleft secondary palate (Hammond et al., 2005; Kochilas et al., 2002; Vitelli et al., 2002).

The 22q11 deletion region comprises more than 30 known genes. Although synteny is not completely conserved between human and mouse, a region of murine chromosome 16 contains a significant number of genes found within the human 22q11 deletion region. This observation prompted the development of mouse models in an attempt to identify the gene or genes responsible for DGS (Scambler, 2000). *TBX1*, a member of the Brachyury-related (T-box) family of transcription factors, has emerged as a good candidate for the DGS because of its chromosomal location (Chieffo et al., 1997) and expression domain (Chapman et al., 1996a; Kochilas et al., 2003; Sauka-Spengler et al., 2002), and because mice generated with a targeted deletion of *Tbx1* have a phenotype resembling that of DGS patients (Jerome and Papaioannou, 2001; Lindsay et al., 2001; Merscher et al., 2001). Supporting this hypothesis, a mutation in *Tbx1* was identified in a case of sporadic DGS (Yagi et al., 2003).

The dentition of DGS subjects is significantly abnormal, and the presence of both hypodontia and enamel defects has been described in several clinical case series (Borglum Jensen et al., 1983; Fukui et al., 2000; Klingberg et al., 2002). The enamel defects range from a delay in mineralization to a more severe and generalized hypomineralization. These anomalies have often been regarded as secondary to the pre-term birth and early systemic insults resulting from congenital heart disease and hypocalcemia that are common in DGS patients. A direct link between impaired *Tbx1* function and enamel defects has not yet been established (Fukui et al., 2000; Klingberg et al., 2002).

Enamel forms via the mineralization of specific enamel matrix proteins that are secreted by highly differentiated dental epithelial cells called ameloblasts. *T-box* genes are involved in the specification of many different cell populations (Papaioannou and Silver, 1998), and *Tbx1* is a candidate regulator of amelogenesis since its expression in the developing mouse molars is restricted to ameloblast progenitors (Mitsiadis et al., 2008c; Zoupa et al., 2006). In addition, forced expression of *Tbx1* in dental explants is capable to activate the expression of the enamel specific *amelogenin* gene (Mitsiadis et al., 2008c). *Tbx1* expression in dental epithelium correlates with cell proliferation events that are under control of FGF signalling (Mitsiadis et al., 2008c). Absence of the *Tbx1* gene in the mouse leads to death at birth (Jerome and Papaioannou, 2001), thus hampering the investigation of the role of this gene in amelogenesis, which occurs mainly at postnatal stages. In addition, the period of tooth development in humans is much longer than in rodents and the effects of a small change in *Tbx1* dosage is more noticeable in humans than in rodents. To overcome these difficulties, we studied the continuously growing mouse incisors which show distinct morphological organization along their anterior–posterior axis with well-defined zones of cell proliferation, cell differentiation and mineral deposition (Mitsiadis et al., 2007). Furthermore, rodent incisors exhibit a characteristic asymmetric deposition of enamel that covers only their labial side, which contains a stem cell niche that constantly supplies ameloblast progenitors (Mitsiadis et al., 2007; Bluteau et al., 2008). In the mature incisors, all ameloblasts that form enamel are derived from cells of this niche, which is located at the cervical loop area. Differential expression of FGF molecules and the *Follistatin* and *Sprouty* genes is associated with the ability of the labial but not the lingual cervical loop to give rise to differentiated ameloblasts (Klein et al., 2008; Wang et al., 2007). Thus to determine the long-term effects of *Tbx1* on cell proliferation, ameloblast differentiation and enamel formation incisor germs were removed from wild-type and *Tbx1* mutant mouse embryos and transplanted into kidney capsules, which offer an ideal environment for the unimpaired development and growth of organs and tissues (Berard, 1975; Morio, 1985).

Here, we provide evidence that *Tbx1* plays a pivotal role in amelogenesis and in the maintenance of epithelial stem cells that are responsible for the continuous supply of ameloblasts in rodent incisors.

Materials and methods

Animals and tissue preparation

Tbx1 mutant mice used in this report have been previously described (Lindsay et al., 2001). *Tbx1* heterozygote mice were crossed and embryos collected at the specified embryonic (E) stage and genotyped. Mice carrying mutant alleles of *Spry2* (Shim et al., 2005) and *Spry4* (Klein et al., 2006) were maintained and genotyped as reported. Age-matched CD1 embryos were used as controls. Swiss and C57Bl/6 wild type mice were also used at embryonic and early postnatal (P) stages (E10 to P2). The age of the mouse embryos was determined according to the appearance of the vaginal plug (day 0) and confirmed by morphological criteria. Animals were killed by cervical dislocation and the embryos were surgically removed in Dulbecco's phosphate-buffered saline (PBS). Dissected heads were fixed overnight at 4 °C in 4% paraformaldehyde (PFA) in PBS. For kidney capsule experiments the incisor germs of E13 to E14 embryos were dissected from the rest of the jaws into Dulbecco's phosphate-buffered saline (PBS) prior transplantation.

Kidney capsule transplantation experiments

All transplantation operations were performed under the appropriate UK Home Office animal licensing procedures. The host animals were anesthetized using pentobarbital (0.8 mg/10 g body weight). Isolated E13–E14 incisor germs were cultured for 2 days in Petri dishes containing media consisting of Dulbecco's Modified Eagle Medium (DMEM; GibcoBRL), 20% foetal calf serum (FCS; GibcoBRL) and 20 U/ml penicillin/streptomycin, as previously reported (Mitsiadis and Drouin, 2008; Mitsiadis et al., 2003, 2008a). After culture the explants were grafted under the kidney capsules of host mice. The transplanted kidneys of the host mice were removed after 28 days and the presence of mature, fully mineralized incisors was determined with radio-graphs (Faxitron, Hewlett Packard). The transplanted tissues were then processed for histological preparation, sectioning, and staining.

Histological procedures

For histological examination the E18.5–E18.75 embryonic tissues were fixed overnight at 4 °C in 4% PFA in PBS. Tissues cultured in kidneys for 28 days were first demineralized in a buffered solution of 4% EDTA, 0.2% PFA at 4 °C for 2 weeks, then dehydrated, embedded in paraffin. 5 μm serial sections were performed. Sirius red and hematoxylin-eosin stainings were performed every other section of non-decalcified (E18.5–E18.75) and decalcified (28 days culture) teeth.

Probes and in situ hybridization

Digoxigenin-labeled (Boehringer Mannheim) sense and antisense riboprobes for mouse *Tbx1* (Chapman et al., 1996b; Mitsiadis and Drouin, 2008; Mitsiadis et al., 2008c), and *amelogenin* (Mitsiadis et al., 2008c) were used. Whole mount *in situ* hybridization on explants and *in situ* hybridization on sections were performed as previously described (Mitsiadis et al., 1995, 2003; Mitsiadis and Drouin, 2008).

Skeletal preparations

Tbx1 mutant and wild type embryos were collected for skeletal analysis at E18.5 and fixed in 95% ethanol for two weeks. Samples were stained for cartilage with 200 μg/ml alcian blue 8 GX (Sigma-Aldrich) in 80% ethanol and 20% glacial acetic acid (BDH) for 3 days at RT.

Thereafter the samples were placed in 95% ethanol for one week, cleared in 1% potassium hydroxide (KOH), and finally stained in 0.1% aqueous alizarin 15 red-s solution (Sigma-Aldrich) for 4 days at RT. Samples were then washed for 30 min in running tap water, decolorized in 20% glycerol (BDH) in 1% KOH, and finally prepared for storage in increasing concentrations of glycerol in 70% ethanol to a final concentration of 100% glycerol.

Mandibular and maxillary incisors were dissected out of the skeletal preparations and photographed in a bright-field Leica stereomicroscope. These incisors were then embedded in paraffin, sectioned and mounted in slides for microscopic examination.

Immunohistochemical analysis of cell proliferation and apoptosis

Proliferating cells were detected using the Proliferating Cell Nuclear Antigen (PCNA) in paraffin sections of incisors from mutant and wild type mice. Immunohistochemistry was carried out essentially according to the manufacturer's instructions (Zymed Laboratories, Hannover, Germany), using the anti-PCNA rabbit polyclonal antibody (1:200; Santa Cruz Biotechnology, USA). Biotinylated secondary antibody against rabbit IgG (1:200) was applied and detected by means of a Vectastain ABC kit (Vector) and diamino-benzidine (DAB; Sigma). Negative control was obtained by omitting the primary antibody.

Apoptosis was detected using a mouse anti-caspase-3 antibody (Transduction Laboratories, Interchim, Montluçon, France). Immunohistochemistry was performed as described previously (Mitsiadis et al., 2008b). Briefly, the anti-caspase-3 antibody (1 μg/ml) was applied on the sections for 30 min at 37 °C. After incubation with the biotinylated secondary antibody, the sections were incubated with peroxidase-conjugated streptavidine for 10 min. Peroxidase was visualized by incubation with 3-amino-9-ethylcarbazole (AEC) reaction solution. In control sections the primary antibody was omitted.

Transmission electron microscopy (TEM)

One mutant incisor grown under kidney capsule, that seemed to have some enamel, as well as two heterozygous incisors and one wild type tooth were selected for TEM examination. Following fixation, incisors were demineralized in 4.13% EDTA (pH 7.2–7.4) at 4 °C for 4 weeks and proceeded for TEM examination. Transplants were, postfixed in 2% Os-tetroxide in 0.2 M Na-cacodylate buffer (pH 7.2–7.4) at room temperature for 45 min and washed thoroughly in the same buffer. For embedding, specimens were dehydrated in ascending grades of alcohol, then transferred to propylene oxide and finally embedded in Epon 812. From the polymerized blocks, sections of about 1 to 2 μm thickness were prepared using histodiamond knives (Diatome, Biel, Switzerland) in a Reichert Ultracut E ultramicrotome (Leica Microsystems, Herbrugg, Switzerland). The sections were stained with periodic acid-Schiff (PAS) and methylene blue-Azur II to select a site for TEM examination. These sites were thin sectioned at a thickness of 60–80 nm using diamond knives (Diatome) in the same Reichert Ultracut E ultramicrotome. The thin sections were collected on copper grids, double contrasted with uranyl acetate and lead citrate, and examined in a Philips EM 400T transmission electron microscope (FEI, Eindhoven, The Netherlands) at an accelerating voltage of 60 kV. Digital micrographs were captured at a resolution of 2272×2272 pixels using a Hamamatsu ORCA-HR camera (Hamamatsu Photonics, Hamamatsu City, Japan) and the program AMT Image Capture Engine 5.42 (Advanced Microscopy Technics, Danvers, MA, USA).

Results

Tbx1 expression in the developing incisor

It was previously reported that *Tbx1*−/− mice exhibit an incisor phenotype (Jerome and Papaioannou, 2001). The continuously erupting incisor of rodents displays distinct

morphological organization along both the labial–lingual and the anterior–posterior axes (Bluteau et al., 2008; Mitsiadis et al., 2007). To better understand and clearly determine the function of *Tbx1* in incisor formation and homeostasis, we first analyzed the expression pattern of the *Tbx1* gene during mouse incisor development.

Initiation of incisor development starts at E10.5–E11 as a local thickening of the oral epithelium that invaginates into the underlying neural crest-derived mesenchyme and progressively acquires the characteristic bud, cap, and bell configurations. Whole-mount *in situ* hybridization analysis showed that *Tbx1* mRNA was present in the oral epithelium from E10. The hybridization signal was weak at E10 in both presumptive incisor and molar areas (Fig. 1A) and became stronger at E10.5–E11, especially in the most distal areas where incisors develop (Figs. 1B and C). No hybridization signal was detected with the sense probe at this or subsequent developmental stages (data not shown).

At E13 (bud stage), *Tbx1* was expressed in epithelial cells in proximity to the dental papilla mesenchyme, while the gene was not detected in cells located in the central part and flanks of the maxillary and mandibular incisor germs (Figs. 1D and E). This restricted expression pattern was maintained in the epithelium during the rotation of the maxillary and mandibular incisors at E14–E14.5 (Figs. 1F–I). At E18.5, *Tbx1* transcripts were detected at the posterior end of the incisor in cells of the inner dental epithelium at the labial side (Fig. 1J). Interestingly, *Tbx1* transcripts were also observed in cells of the outer dental epithelium at the very posterior end of the incisor. The gene was absent from the rest of the dental epithelium extending anteriorly (i.e. preameloblasts, ameloblasts, outer dental epithelial cells) on the labial side, and from the dental epithelium (i.e. inner and outer dental epithelia) on the lingual side (Fig. 1J).

Altered growth and mineralization in developing Tbx1−/− incisors

The expression pattern of *Tbx1* in the incisor suggests that this transcription factor has an important role in the developing incisor, and more precisely in amelogenesis. Indeed, the incisors of *Tbx1*−/− mice were significantly shorter than in wild-type mice, and furthermore, the enamel was absent in most of these mutant incisors (Figs. 2–5).

At E18.5, the incisor is at the bell stage and epithelial cells (inner dental epithelium) facing the dental papilla mesenchyme differentiate into preameloblasts. Incisors were carefully extracted from the mandible and maxilla of skeletal preparations from E18.5 *Tbx1*−/− mice and were compared to incisors from E18.5 wild type littermates, to evaluate their size and level of mineralization macroscopically. This examination revealed that both the growth and mineral deposition processes of the mutant incisors were altered. The *Tbx1*−/− teeth were smaller and less mineralized than those of the wild-type mice (Fig. 2A), and the epithelial layer responsible for enamel secretion (Fig. 2A, green arrows) was always significantly thinner in the mutant incisors when compared to that of the normal incisors. However, length reduction/hypoplasticity and mineral deposition were more prominent in the maxillary mutant incisors (Fig. 2A, orange arrows). Furthermore, mineral deposition ranged from reduced/low levels to nonexistent in the maxillary mutant incisors (Fig. 2A, black arrows). It is noteworthy that the labial–lingual asymmetry of hard tissue deposition was also altered in the *Tbx1*−/− incisors. In the developing incisors of wild-type mouse embryos, the process of hard tissue formation is more advanced on the labial side when compared to the lingual side (Fig. 2A, green line). This asymmetry was not evident in the mutant incisors, where often the deposition of minerals was identical on both lingual and labial sides. Longitudinal sections of the mutant maxillary incisors (Fig. 2B) showed that minerals are deposited in a non-structured, sporadic way, leading thus to un-organized mineral structure in the labial side (Figs. 2D–F) as compared to the lingual side (Fig. 2C).

The histological examination of E18.5–E18.75 *Tbx1*−/− incisors showed a phenotypic variability ranging from severe to mild manifestations (Fig. 3), due to the different degrees of penetrance. Although odontoblast differentiation and dentin matrix secretion occur normally, the differentiation of preameloblasts into ameloblasts appears to be defective: we were not able to detect functional ameloblasts and enamel in the *Tbx1*−/− incisors (Figs. 3A–C, F–J). In some *Tbx1*−/− incisors inner dental epithelial cells of the labial side at the median and anterior parts were tiny and exhibited a spherical shape (Figs. 3H, J), resembling the epithelial cells of the lingual side (Fig. 3H). A characteristic feature of the maxillary *Tbx1*−/− incisors was that the cervical loop on the labial side regressed considerably, while the cervical loop at the lingual side expanded significantly (Figs. 3A, B), when compared with the equivalent areas of the maxillary *Tbx1*+/− incisors (Fig. 3D). A more detailed observation showed that the structure of the cervical loop at the labial side was severely disturbed in the *Tbx1*−/− incisors (Fig. 3L), but not the *Tbx1*+/− incisors (Fig. 3K).

Mature Tbx1−/− incisors lack enamel

In order to further understand the functional role of *Tbx1* in incisor development, and to overcome the problem of the early lethality of the *Tbx1*−/− mice, we used the kidney transplantation technique. This technique allowed a long-term culture (i.e. 28 days) of isolated incisor germs from E13–E14 *Tbx1*−/−, *Tbx1*+/−, and wild-type mouse embryos. These incisor germs were transferred to kidney capsules and their development assayed (Figs. 4A–C). From a total of 5 experiments, 3 wild-type, 4 *Tbx1*+/−, and 8 *Tbx1*−/− incisors were grown to full maturity under these conditions and recovered for further analysis. X-ray imaging was used to determine their degree of mineralization (Figs. 4D–G). It was evident from these radiographs that the radio-opacity of the mineralized tissues was more pronounced in the wild-type and *Tbx1*+/− incisors (Fig. 4G) than in the *Tbx1*−/− incisors (Figs. 4D–F). Increased radio-opacity was observed on the labial side of the wild type and *Tbx1*+/− incisors (Fig. 4G), while radio-opacity was equal on the lingual and labial sides of the *Tbx1*−/− incisors (Figs. 4D–F). Identical radio-opacity indicates that there is only dentin deposition on the lingual and labial sides of the mutant incisors, and thus represents the absence of enamel on their labial side. This was confirmed by the observation that the characteristic yellow color of rodent incisors enamel was not detected in the *Tbx1*−/− teeth grown in kidneys (Figs. 4H–J).

Histological examination demonstrated that wild-type and *Tbx1*+/− incisors develop normally in kidney-capsule explants and maintain their capacity to form enamel on their labial side (Fig. 5A, red boxes). The shape of the functional ameloblasts followed the various stages of enamel secretion and exhibited either a tall columnar shape or a low cubical profile. The development of the lingual side of these incisors was not disturbed as well (Fig. 5A, green box), and as expected, ameloblasts and enamel were absent on the lingual side. In contrast, we were not able to detect preameloblasts, ameloblasts, and enamel in the *Tbx1*−/− incisors (Fig. 5B). Epithelial cells of the labial side were tiny and exhibited a flat or spherical shape (Fig. 5B, red boxes), closely resembling the cells overlying the hard tissue (i.e. cementum) on the lingual side (Fig. 5B, green boxes). In addition, ameloblast precursors, which are normally detected in the cervical loop on the labial side, were not present in the mutant incisors (Fig. 5B, red box in left). A characteristic feature of the *Tbx1*−/− incisors was that the cervical loop on the labial side regressed considerably. This had as a consequence the reversal of the normal incisor morphology, with a lingual side longer than the labial side (compare Fig. 5A with Fig. 5B). Finally, the mutant incisors showed the same degree of dentin deposition on both labial and lingual sides, while in the wild-type dentin was thicker on the labial side when compared to the lingual side (Fig. 5A). In contrast, the dentin in the *Tbx1*−/− teeth was much thicker than in the wild type and *Tbx1*+/− incisors (compare Fig. 5A with Fig. 5B).

Electron microscopy examination of Tbx1−/−, Tbx1+/− and wild type mature incisors

Only one out of the eight *Tbx1* mutant incisors grown under kidney capsule seemed to have enamel deposition, and it was used to examine the ultrastructural properties of the enamel. When ameloblasts were present in mature mutant incisors these contained abnormal vacuoles that were concentrated in the secreting front and that were not present in other cell layers (Fig. 6, red arrows). The organelles and Tomes' processes of the ameloblasts were very disorganized, partly disrupted and in a process of apparent disintegration, giving the impression of dying cells. Cytoplasmic vacuoles were also present in ameloblasts of the heterozygote incisors, but they were much less prominent and occurred only occasionally in wild type specimens.

Cell apoptosis and proliferation in incisors of Tbx1 mutants

Since incisor development and morphogenesis require a tight balance between cell proliferation and apoptosis, we asked whether these two events were abnormal in the incisors of *Tbx1* null mutants. Despite the absence of ameloblasts and the reduced length of the *Tbx1*−/− incisors, apoptosis was not altered in incisors of E18.5 embryos. Apoptotic cells were scarcely observed in the dental epithelium (Fig. 7), and few apoptotic cells were detected in the alveolar bone (Fig. 7). No apoptosis was detected in *Tbx1*−/− incisors cultured in kidneys, as well as in control sections (data not shown).

In contrast, cell proliferation was abnormal in the epithelium of the *Tbx1*−/−incisors. This was more pronounced in the cervical loop area on the labial side, which contains a population of actively proliferating cells (Figs. 8A and B). In the mutant incisors, the total number of proliferating cells was decreased dramatically (by approximately 60%) in the cervical loop. A more severe effect was observed in the layer of presumptive inner dental epithelium, which contains the ameloblast progenitors, where cell proliferation was undetectable (Figs. 8A and B). In contrast, intense cell proliferation was detected in both the cervical loop area and the inner dental epithelium of wild type incisors (Figs. 8C and D).

Amelogenin expression in incisors of Tbx1 mutants

Amelogenin is a marker of ameloblast differentiation and initiation of enamel formation. In our previous studies we showed that *Tbx1* misexpression induced *amelogenin* expression in the mouse mandible (Mitsiadis et al., 2008c), thus showing that a close link exists between the *Tbx1* and *amelogenin* genes. Thus, we asked whether *Tbx1* deletion could affect *amelogenin* expression in incisors.

In situ hybridization in sections of E18.5–E18.75 wild type and Tbx+/− mouse embryos showed that *amelogenin* was strongly expressed in cells of the inner dental epithelium that differentiate into ameloblasts (Fig. 9A, and data not shown). In contrast, the *amelogenin* gene was either absent or weakly expressed in incisors of *Tbx1* null mutants (Fig. 9A). It is noteworthy that weaker expression was observed in the maxillary incisors (Fig. 9A).

In teeth that were cultured under kidney capsule for 28 days, *amelogenin* transcripts were detected in ameloblasts of the wild type and *Tbx1*+/− incisors, while transcripts were not found in mature *Tbx1*−/− incisors (Fig. 9B, and data not shown).

Genetic interactions between Sprouty, Tbx1, and amelogenin genes in incisors

Sprouty genes encode antagonists of receptor tyrosine kinase signalling and have been shown to prevent the generation of ameloblasts in the lingual epithelium of incisors by antagonizing an epithelial–mesenchymal FGF signalling loop (Klein et al., 2008). Loss of *Sprouty* gene function leads to bilateral enamel deposition as a result of ectopic generation of ameloblasts from stem cells in the lingual cervical loop. In our previous work we showed that *Tbx1* is expressed in response to FGF signals in ameloblast progenitor cells (Mitsiadis et al., 2008c).

To further analyze the involvement of FGF signalling in *Tbx1* induction and/or maintenance, we studied and compared the expression of *Tbx1* in incisors from wild type embryos with those from embryos carrying three *Sprouty* null alleles (*Spry2+/−;Spry4−/−* mice). In E16.5 wild type incisors, *Tbx1* was only expressed in the labial epithelium and cervical loop (Fig. 10A). In the E16.5 *Spry2+/−;Spry4−/−* mutant incisors, *Tbx1* was ectopically expressed on the lingual side, but was restricted to the posterior end of the tooth (Fig. 10B). To determine if this ectopic *Tbx1* expression was linked to the differentiation of inner dental epithelium cells into ameloblasts we examined the expression of *amelogenin* in the incisors of the *Sprouty* mutants. *Amelogenin* expression was detected in both labial and lingual sides of the postnatal day 2 incisors of the *Sprouty* mutants, thus confirming the presence of mature ameloblasts on the lingual side (Fig. 10C).

Discussion

Tooth development depends on sequential and reciprocal interactions between cells of the oral epithelium and cranial neural crest-derived mesenchyme (Cobourne and Mitsiadis, 2006; Lumsden, 1988; Mitsiadis, 2001). Cells from the dental epithelium differentiate into ameloblasts and secrete the organic matrix of enamel, which is a highly mineralized tissue unique to teeth. Specific secreted signalling molecules and transcription factors are required for odontogenesis at each stage of tooth development (reviewed by Mitsiadis, 2001; Tucker and Sharpe, 2004). Our previous studies have shown that expression of the transcription factor *Tbx1* is correlated with epithelial cell proliferation and ameloblast differentiation, and, furthermore, activates *amelogenin* expression in the developing mouse molars (Mitsiadis et al., 2008c).

In humans and most mammals, whose teeth do not undergo continuous eruption, ameloblasts synthesize, deposit, mineralize and mature the enamel matrix, and finally regress and disappear when the tooth crowns emerge into the oral cavity. In contrast, rodent incisors erupt continuously, a process that involves the generation of new ameloblasts for the *de novo* formation and deposition of enamel. This continuous process is due to the presence of a population of epithelial stem cells that are located in the apical part of the incisor, the cervical loop area (Harada et al., 1999,2002;Mitsiadis et al., 2007). Stem cells from the cervical loop generate transit amplifying progenitor cells that differentiate into all epithelial cell types of the tooth, including the ameloblasts (Bluteau et al., 2008;Mitsiadis et al., 2007). Disruption or damage of this area results in the arrest of new enamel formation (Merzel and Novaes, 2006). Therefore, the rodent incisor constitutes a unique model of amelogenesis involving well-defined compartments of cell proliferation, differentiation and maturation.

Another intriguing aspect of the rodent incisor is that enamel is present only on the labial side, while dental epithelial cells of the lingual side do not differentiate into ameloblasts and thus cannot synthesize enamel matrix. Ameloblast progenitors are morphologically indistinguishable from all other immature dental epithelial cells. Our studies suggest that *Tbx1* expression is required in the progenitors of ameloblasts as opposed to the rest of the dental epithelium. Indeed, *Tbx1* is expressed in cells of the cervical loop and inner enamel epithelium (i.e. the ameloblast precursors) on the labial side of the incisor. In contrast, *Tbx1* is not expressed in epithelial cells of the lingual side where enamel is not formed. Therefore, it is quite possible that *Tbx1* plays a pivotal role in the specification and proliferation of the restricted dental cell population that is responsible for the generation of ameloblasts.

Epithelial cells such as the ameloblast progenitors actively proliferate under the control of *Tbx1* (Mitsiadis et al., 2008c; Xu et al., 2007). Indeed, proliferation of epithelial cells was greatly reduced in the *Tbx1−/−* incisors when compared to the incisors of wild type animals. This disturbance of cell proliferation was restricted to ameloblast precursors that normally

express *Tbx1*, and thus is possibly responsible for the enamel defects in the *Tbx1* mutant incisors. Mutant incisors grown to maturity in kidney capsules were hypoplastic and exhibited a deficiency in mineral deposition. Although a thin layer of enamel and some ameloblasts were present in very few mutant incisors, the majority of these teeth lacked enamel, ameloblasts, and their precursors. In the rare mutant incisors that exhibited enamel formation, electron microscopy revealed the presence of uncharacteristic vacuoles at the secreting poles of the ameloblasts and a defective enamel structure. Vacuoles were also present in the ameloblasts of the heterozygote incisors but their size and number were smaller than in the *Tbx1*−/− incisors, thus indicating that the heterozygote mice might also exhibit a mild enamel phenotype. Taken together these findings clearly show that *Tbx1* is necessary for the proliferation, maintenance and homeostasis of the ameloblastic lineage.

Large variations in both tooth size and degree of mineralization have been observed in DGS patients (Borglum Jensen et al., 1983; Fukui et al., 2000; Klingberg et al., 2002). In addition to the visible enamel defects, histological examinations have demonstrated a significant enhancement in the deposition of dentin (Fukui et al., 2000), which is synthesized by the mesenchyme-derived odontoblasts. Similarly, the anomalies in the incisors of the *Tbx1*−/− mice were not limited to their epithelial component, as indicated by the increased thickness of dentin. However, dental abnormalities in DGS patients are less severe than those observed in the teeth of the *Tbx1*−/− mice. This could be explained by the fact that DGS is a haploinsufficiency condition, whereas we studied mice that were lacking all *Tbx1* function.

Incisors from the *Tbx1*−/− mice showed variable degrees of hypomineralization and hypoplasticity. This phenotypic variability could be the result of incomplete penetrance. Alternatively, other transcription factors may partly compensate for the loss of *Tbx1*. An additional phenotypic variability was noticed with respect to the maxillary *Tbx1*−/− incisors, which consistently were more severely affected than those of the mandible. These jaw-specific differences are consistent with the observation that the development of the maxillary teeth is delayed when compared to the development of the mandibular teeth. For example, E18.5 mandibular incisors are longer and contain more hard tissue deposits than the maxillary incisors, which are shorter and less mineralized.

In the incisors of the *Tbx1*−/− mice the labial–lingual asymmetry of hard tissue formation was also affected. Normally, the processes of cytodifferentiation and mineralized tissue deposition are more advanced on the labial as compared to the lingual side of the developing mouse incisor. However, this difference was not evident in the incisors of the mutant mice, where the deposition of minerals was symmetric on the lingual and labial side. This modification implies that *Tbx1* deletion can cause a deposition imbalance, presumably due to a cellular disruption and/or dysfunction in the epithelium of the labial side, where *Tbx1* is normally expressed.

The process of enamel formation involves the synthesis and secretion of several extracellular enamel matrix proteins. The most abundant of these proteins is amelogenin (Zeichner-David et al., 1997), which is considered as the best marker for ameloblast differentiation and initiation of enamel formation. We have recently shown that forced *Tbx1* expression is sufficient to induce *amelogenin* expression in the odontogenic epithelium (Mitsiadis et al., 2008c), indicating that *amelogenin* expression is under the control of *Tbx1*. However, in the present study we detected low levels of *amelogenin* in a few of the E18.5 *Tbx1*−/− incisors. While the levels of *amelogenin* expression were similar in the developing maxillary and mandibular incisors of the wild type mice, in the developing incisors of the *Tbx1* mutants expression ranged from low levels in the mandibular incisors to non-detectable levels in most of the maxillary incisors. This could be the result of variability in penetrance, which may also affect the severity of the tooth phenotype. Phenotype variability in teeth or other organs, in the Tbx1 mutants and the DGS patients, may suggest that there is a threshold level associated with unstable balance,

which can be perturbed by chance events (Zhang and Baldini, 2008). Alternatively, it is also possible that *Tbx1* affects *amelogenin* expression indirectly by playing a role in maintenance and induction of differentiation of the ameloblast precursors (i.e. inner dental epithelial cells). *Amelogenin* was not expressed at all in the mature *Tbx1−/−* incisors that were grown in kidney capsules. This is reflected by the absence of enamel in these teeth, and suggests that cell fate determination in the incisors of the mutant mice was compromised. The absence of *amelogenin* from the *Tbx1−/−* incisors cultured in kidney capsules could be explained by the fact that during the culture period (i.e. 28 days) the very first formed preameloblasts, which expressed weakly the *amelogenin* gene at E18.5, have either already disappeared by apoptosis or changed their fate. In contrast to the wild-type incisors, cells from the cervical loop of the *Tbx1−/−* incisors are not able to differentiate into preameloblasts/ameloblasts and therefore do not express *amelogenin*.

Several studies indicate that FGF and BMP signalling are required for the maintenance of ameloblast precursors in the incisors (Klein et al., 2008; Mitsiadis et al., 2008a; Wang et al., 2007; Wang et al., 2004). We recently demonstrated that mesenchyme-derived FGF molecules are important for the maintenance of *Tbx1* expression in the dental epithelium (Mitsiadis et al., 2008c). Furthermore, studies in other developing organs have shown that FGF molecules form a regulatory loop with *Tbx1* (Vitelli et al., 2002). It was therefore important for us to determine whether FGF signalling induced *Tbx1* expression in the epithelial progenitor cells of incisors. We therefore examined the incisors of mice carrying null alleles of *Sprouty* genes, which are antagonists of FGF signalling. These mice are hypersensitive to FGF and other receptor-tyrosine kinase signalling because they have decreased dosage of the FGF antagonists. We have previously shown that the incisors of *Spry4−/−;Spry2+/−* mice are covered by enamel on both labial and lingual sides (Klein et al., 2008). In the present study, we found that *Tbx1* and *amelogenin* were ectopically expressed on the lingual side of these mutant incisors, indicating that upregulation of FGF signalling leads to ectopic *Tbx1* expression and confirming our previous findings that *Tbx1* is a target of FGF signalling. It is worth noting that the cervical loop on the lingual side of the *Spry4−/−;Spry2+/−* incisors was larger than that of the normal incisors. This difference in size may result in part from increased cell proliferation owing to the ectopic expression of *Tbx1* on the lingual side of the mutant incisors. Thus, the results from our studies on the *Spry4−/−;Spry2+/−* mice reinforce our assumption that *Tbx1* plays an important role in the proliferation and maintenance of the ameloblast precursors by mediating the function of FGF molecules.

In conclusion, the incisors of the *Tbx1−/−* mice showed diverse anomalies, with the most striking being the lack of enamel. These phenotypes resulted from decreased cell proliferation and *amelogenin* expression, as well as from various defects in cytodifferentiation and mineralization (Fig. 11). Hence, the phenotypes of the *Tbx1−/−* incisors might help to better understand dental anomalies observed in DGS patients. However, penetrance variability makes the phenotypic determination elusive and the responsible mechanisms complicated to determine.

Acknowledgments

We would like to thank Professor Antonio Baldini from the Institute of Genetics and Biophysics of Napoli, Professor Peter Scambler and Miss Catherine Roberts from UCL London, for making available the Tbx1 mutant mice and their help in starting the Tbx1 colony. We are also grateful to Professor Gail Martin for providing the Sprouty mutant mice. This work was supported by grants from the University of Zurich (T.M.), Swiss National Foundation (T.M.), Guy's and St Thomas' Charity Foundation (T.M., J.C., A.S.T.), and NIH (K08-DE017654) (O.K.).

References

Berard R. Studies of the development of the molar root experimentally grafted under the kidney capsule of the rat. Actual Odontostomatol. (Paris) 1975;110:285–296. [PubMed: 1190010]

Bluteau G, Luder HU, De Bari C, Mitsiadis TA. Stem cells for tooth engineering. Eur. Cell Mater 2008;16:1–9. [PubMed: 18671204]

Jensen, S. Borglum; Jacobsen, P.; Rotne, L.; Enk, C.; Illum, F. Oral findings in DiGeorge syndrome. Int. J. Oral Surg 1983;12:250–254. [PubMed: 6418672]

Chapman DL, Agulnik I, Hancock S, Silver LM, Papaioannou VE. Tbx6, a mouse T-Box gene implicated in paraxial mesoderm formation at gastrulation. Dev. Biol 1996a;180:534–542. [PubMed: 8954725]

Chapman DL, Garvey N, Hancock S, Alexiou M, Agulnik SI, Gibson-Brown JJ, Cebra-Thomas J, Bollag RJ, Silver LM, Papaioannou VE. Expression of the T-box family genes, *Tbx1–Tbx5*, during early mouse development. Dev. Dyn 1996b;206:379–390. [PubMed: 8853987]

Chieffo C, Garvey N, Gong W, Roe B, Zhang G, Silver L, Emanuel BS, Budarf ML. Isolation and characterization of a gene from the DiGeorge chromosomal region homologous to the mouse Tbx1 gene. Genomics 1997;43:267–277. [PubMed: 9268629]

Cobourne MT, Mitsiadis T. Neural crest cells and patterning of the mammalian dentition. J. Exp. Zoolog. B Mol. Dev. Evol 2006;306:251–260.

Fukui N, Amano A, Akiyama S, Daikoku H, Wakisaka S, Morisaki I. Oral findings in DiGeorge syndrome: clinical features and histologic study of primary teeth. Oral Surg. Oral Med. Oral Pathol. Oral Radiol. Endod 2000;89:208–215. [PubMed: 10673658]

Hammond P, Hutton TJ, Allanson JE, Buxton B, Campbell LE, Clayton-Smith J, Donnai D, Karmiloff-Smith A, Metcalfe K, Murphy KC, Patton M, Pober B, Prescott K, Scambler P, Shaw A, Smith AC, Stevens AF, Temple IK, Hennekam R, Tassabehji M. Discriminating power of localized three-dimensional facial morphology. Am. J. Hum. Genet 2005;77:999–1010. [PubMed: 16380911]

Harada H, Kettunen P, Jung HS, Mustonen T, Wang YA, Thesleff I. Localization of putative stem cells in dental epithelium and their association with Notch and FGF signaling. J. Cell Biol 1999;147:105–120. [PubMed: 10508859]

Harada H, Toyono T, Toyoshima K, Yamasaki M, Itoh N, Kato S, Sekine K, Ohuchi H. FGF10 maintains stem cell compartment in developing mouse incisors. Development 2002;129:1533–1541. [PubMed: 11880361]

Jerome LA, Papaioannou VE. DiGeorge syndrome phenotype in mice mutant for the T-box gene, Tbx1. Nat. Genet 2001;27:286–291. [PubMed: 11242110]

Klein OD, Minowada G, Peterkova R, Kangas A, Yu BD, Lesot H, Peterka M, Jernvall J, Martin GR. Sprouty genes control diastema tooth development via bidirectional antagonism of epithelial–mesenchymal FGF signaling. Dev. Cell 2006;11:181–190. [PubMed: 16890158]

Klein OD, Lyons DB, Balooch G, Marshall GW, Basson MA, Peterka M, Boran T, Peterkova R, Martin GR. An FGF signaling loop sustains the generation of differentiated progeny from stem cells in mouse incisors. Development 2008;135:377–385. [PubMed: 18077585]

Klingberg G, Oskarsdottir S, Johannesson EL, Noren JG. Oral manifestations in 22q11 deletion syndrome. Int. J. Paediatr. Dent 2002;12:14–23. [PubMed: 11853243]

Kochilas L, Merscher-Gomez S, Lu MM, Potluri V, Liao J, Kucherlapati R, Morrow B, Epstein JA. The role of neural crest during cardiac development in a mouse model of DiGeorge syndrome. Dev. Biol 2002;251:157–166. [PubMed: 12413905]

Kochilas LK, Potluri V, Gitler A, Balasubramanian K, Chin AJ. Cloning and characterization of zebrafish tbx1. Gene Expr. Patterns 2003;3:645–651. [PubMed: 12972000]

Lindsay EA, Vitelli F, Su H, Morishima M, Huynh T, Pramparo T, Jurecic V, Ogunrinu G, Sutherland HF, Scambler PJ, Bradley A, Baldini A. Tbx1 haploinsufficiency in the DiGeorge syndrome region causes aortic arch defects in mice. Nature 2001;410:97–101. [PubMed: 11242049]

Lumsden AG. Spatial organization of the epithelium and the role of neural crest cells in the initiation of the mammalian tooth germ. Development 1988;103(Suppl):155–169. [PubMed: 3250849]

Merscher S, Funke B, Epstein JA, Heyer J, Puech A, Lu MM, Xavier RJ, Demay MB, Russell RG, Factor S, Tokooya K, Jore BS, Lopez M, Pandita RK, Lia M, Carrion D, Xu H, Schorle H, Kobler JB, Scambler P, Wynshaw-Boris A, Skoultchi AI, Morrow BE, Kucherlapati R. TBX1 is responsible for

cardiovascular defects in velo-cardio-facial/DiGeorge syndrome. Cell 2001;104:619–629. [PubMed: 11239417]

Merzel J, Novaes PD. Development of functional dentin incisors after a partial resection of the odontogenic organ of rat incisors. Arch. Oral Biol 2006;51:825–835. [PubMed: 16730636]

Mitsiadis, T. Bases moléculaires du développement dentaire. In: Piette, E.; Goldberg, M., editors. La Dent Normale Et Pathologique. De Boeck-Université Press; 2001. p. 19-38.

Mitsiadis TA, Drouin J. Deletion of the Pitx1 genomic locus affects mandibular tooth morphogenesis and expression of the *Barx1* and *Tbx1* genes. Dev. Biol 2008;313:887–896. [PubMed: 18082678]

Mitsiadis TA, Salmivirta M, Muramatsu T, Muramatsu H, Rauvala H, Lehtonen E, Jalkanen M, Thesleff I. Expression of the heparin-binding cytokines, midkine (MK) and HB-GAM (pleiotrophin) is associated with epithelial–mesenchymal interactions during fetal development and organogenesis. Development 1995;121:37–51. [PubMed: 7867507]

Mitsiadis TA, Angeli I, James C, Lendahl U, Sharpe PT. Role of Islet1 in the patterning of murine dentition. Development 2003;130:4451–4460. [PubMed: 12900460]

Mitsiadis TA, Barrandon O, Rochat A, Barrandon Y, De Bari C. Stem cell niches in mammals. Exp. Cell Res 2007;313:3377–3385. [PubMed: 17764674]

Mitsiadis TA, Caton J, De Bari C, Bluteau G. The large functional spectrum of the heparin-binding cytokines MK and HB-GAM in continuously growing organs: the rodent incisor as a model. Dev. Biol 2008a;320:256–266. [PubMed: 18582856]

Mitsiadis TA, De Bari C, About I. Apoptosis in developmental and repair-related human tooth remodeling: a view from the inside. Exp. Cell Res 2008b;314:869–877. [PubMed: 18054913]

Mitsiadis TA, Tucker AS, De Bari C, Cobourne MT, Rice DP. A regulatory relationship between Tbx1 and FGF signaling during tooth morphogenesis and ameloblast lineage determination. Dev. Biol 2008c;320:39–48. [PubMed: 18572158]

Morio I. Recombinant study of the mouse molar cervical loop and dental papilla by renal transplantation. Arch. Oral Biol 1985;30:557–561. [PubMed: 3864405]

Papaioannou VE, Silver LM. The T-box gene family. BioEssays 1998;20:9–19. [PubMed: 9504043]

Sauka-Spengler T, Le Mentec C, Lepage M, Mazan S. Embryonic expression of Tbx1, a DiGeorge syndrome candidate gene, in the lamprey *Lampetra fluviatilis*. Gene Expr. Patterns 2002;2:99–103. [PubMed: 12617845]

Scambler PJ. The 22q11 deletion syndromes. Hum. Mol. Genet 2000;9:2421–2426. [PubMed: 11005797]

Shim K, Minowada G, Coling DE, Martin GR. Sprouty2, a mouse deafness gene, regulates cell fate decisions in the auditory sensory epithelium by antagonizing FGF signaling. Dev. Cell 2005;8:553–564. [PubMed: 15809037]

Tucker A, Sharpe P. The cutting-edge of mammalian development; how the embryo makes teeth. Nat. Rev., Genet 2004;5:499–508. [PubMed: 15211352]

Vitelli F, Taddei I, Morishima M, Meyers EN, Lindsay EA, Baldini A. A genetic link between Tbx1 and fibroblast growth factor signaling. Development 2002;129:4605–4611. [PubMed: 12223416]

Wang XP, Suomalainen M, Jorgez CJ, Matzuk MM, Werner S, Thesleff I. Follistatin regulates enamel patterning in mouse incisors by asymmetrically inhibiting BMP signaling and ameloblast differentiation. Dev. Cell 2004;7:719–730. [PubMed: 15525533]

Wang XP, Suomalainen M, Felszeghy S, Zelarayan LC, Alonso MT, Plikus MV, Maas RL, Chuong CM, Schimmang T, Thesleff I. An integrated gene regulatory network controls stem cell proliferation in teeth. PLoS Biol 2007;5:e159. [PubMed: 17564495]

Xu H, Viola A, Zhang Z, Gerken CP, Lindsay-Illingworth EA, Baldini A. Tbx1 regulates population, proliferation and cell fate determination of otic epithelial cells. Dev. Biol 2007;302:670–682. [PubMed: 17074316]

Yagi H, Furutani Y, Hamada H, Sasaki T, Asakawa S, Minoshima S, Ichida F, Joo K, Kimura M, Imamura S, Kamatani N, Momma K, Takao A, Nakazawa M, Shimizu N, Matsuoka R. Role of TBX1 in human del22q11.2 syndrome. Lancet 2003;362:1366–1373. [PubMed: 14585638]

Zeichner-David M, Vo H, Tan H, Diekwisch T, Berman B, Thiemann F, Alcocer MD, Hsu P, Wang T, Eyna J, Caton J, Slavkin HC, MacDougall M. Timing of the expression of enamel gene products during mouse tooth development. Int. J. Dev. Biol 1997;41:27–38. [PubMed: 9074935]

Zhang Z, Baldini A. In vitro response to high-resolution variation of Tbx1 mRNA dosage. Hum. Mol. Genet 2008;17:150–157. [PubMed: 17916582]

Zoupa M, Seppala M, Mitsiadis T, Cobourne MT. Tbx1 is expressed at multiple sites of epithelial–mesenchymal interaction during early development of the facial complex. Int. J. Dev. Biol 2006;50:504–510. [PubMed: 16586352]

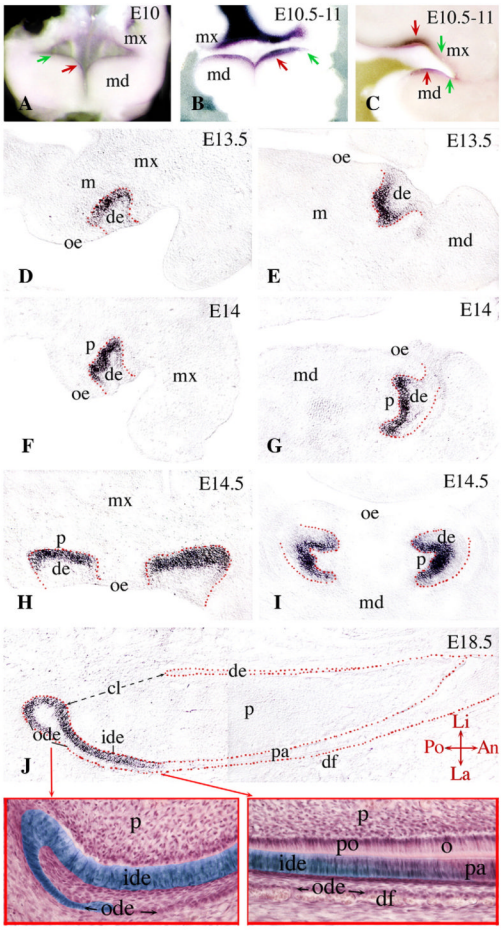

Fig. 1.

Patterns of *Tbx1* expression in oral epithelium and in developing incisors. Whole-mount in situ hybridization (A–C) and in situ hybridization on cryosections (D–J) using a digoxigenin-labeled probe. Longitudinal (D–G, J) and frontal (H, I) sections. (A–B) Frontal (A, B) and lateral (C) views of E10 and E10.5–11 mouse embryos showing *Tbx1* mRNA expression (violet color) in oral epithelium. Red and green arrows indicate the incisor and molar growing areas respectively. Note that *Tbx1* expression is stronger in the incisor areas. (D–J) *Tbx1* expression in developing incisors during the bud (D, E), cap (F–I) and bell (J) stages. Boxes in panel J represent high magnifications of selected areas of hematoxylin/eosin stained sections. The blue color indicates territories of *Tbx1* expression. Abbreviations: An, anterior part; cl, cervical loop; d, dentin; de, dental epithelium; df, dental follicle; ide, inner dental epithelium; La, labial part; Li, lingual part; m, mesenchyme; md, mandible; mx, maxilla; o, odontoblasts; ode, outer dental epithelium; oe, oral epithelium; p, dental papilla; pa, preameloblasts; po, preodontoblasts; Po, posterior part.

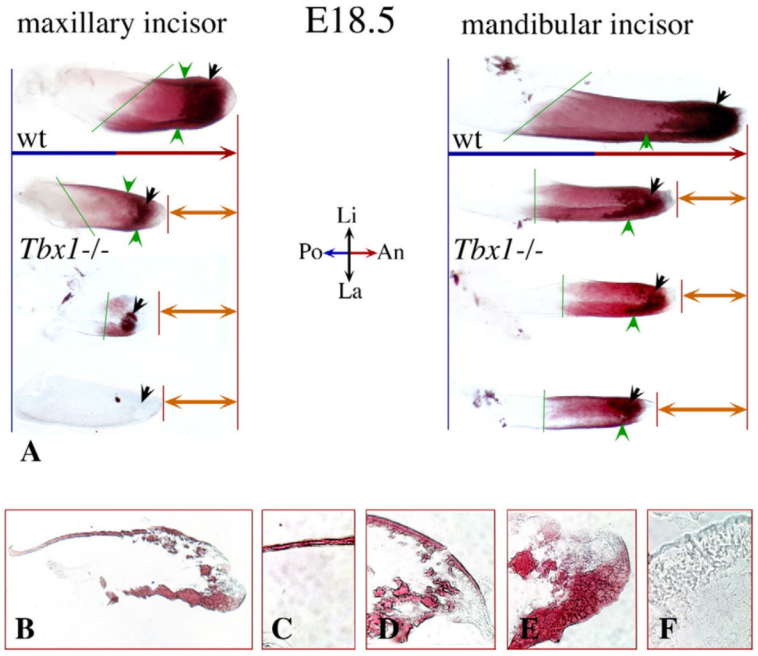

Fig. 2.

Incisors (intact and sectioned) isolated from skeletal preparations of E18.5 wild-type and *Tbx1* −/− mouse embryos. (A) Maxillary (left) and mandibular (right) E18.5 wild-type (wt) incisors (top panel) and *Tbx1*−/− incisors (three bottom incisors). Mineral matrix deposition in red color (alizarin red staining). The double-headed orange arrows indicate the difference in size between the normal incisors and the mutant incisors. Black arrowheads indicate the area of the incisor where minerals start to deposit (i.e. mineralization front), and green arrowheads show the layer of dental epithelium. The green line at the posterior end of the incisors represents the mineralization gradient on the labial and lingual sides. (B–F) Sections of the above mutant incisors showing variations in mineral deposition and organization (red color). (B) Section of an entire *Tbx1*−/− incisor. (C) High magnification of the lingual side. (D–F) High magnifications of the anterior parts of three mutant incisors. Abbreviations: An, anterior part; La, labial side; Li, lingual side; Po, posterior part.

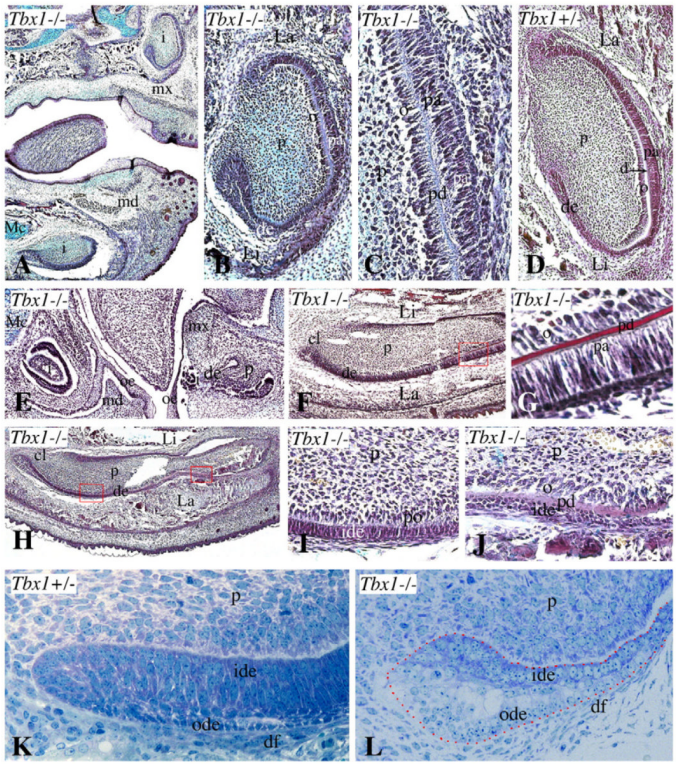

Fig. 3.

Histological examination of various *Tbx1* mutant incisors. Histological preparations of *Tbx1* −/− (A–C, E–J, L) and *Tbx1*+/− (D, K) E18.5 incisors. Longitudinal sections. Hematoxylin-eosin (A–C), Sirius red (D–J), and periodic acid-Schiff and methylene blue-Azur II (K, L) stainings. (A) Maxillary and mandibular incisors (i) in *Tbx1*−/− mouse. (B) Higher magnification of the maxillary incisor. Note the thin cervical loop epithelium at the labial side (La) and the thick equivalent area at the lingual side (Li). (C) Higher magnification of the cytodifferentiation area. Only preameloblasts (pa) are visible. The enamel is also absent. (D) Maxillary incisor. Note the thick cervical loop epithelium at the labial side and the thin equivalent part at the lingual side. (E) Massive necrotic areas in all tissues of the craniofacial complex. (F) Mandibular incisor. The red frame represents the blow up area of the next figure. (G) High magnification showing the deposition of predentin and the existence of preameloblasts in the anterior part of the incisor. No enamel is visible. (H) Another mandibular incisor. Red frames represent blow up areas of the next two figures. (I) Start of predentin deposition by preodontoblasts (po) at the transition part of the incisor. Inner dental epithelial cells (ide), but not preameloblasts (pa), are visible. (J) Anterior part of the incisor. Odontoblasts (o) and predentin/dentin (pd) are visible. Note in the epithelium the existence of small round cells instead of inner dental epithelial cells/preameloblasts. (K) High magnification of the cervical loop area. (L) Disintegration of epithelial cells at the cervical loop of *Tbx1*−/− incisors. Red dots indicate the form of dental epithelium. Additional abbreviations: cl, cervical loop; d, dentin; de, dental epithelium; df, dental follicle; md, mandible; mx, maxilla; ode, outer dental epithelium; oe, oral epithelium; p, pulp.

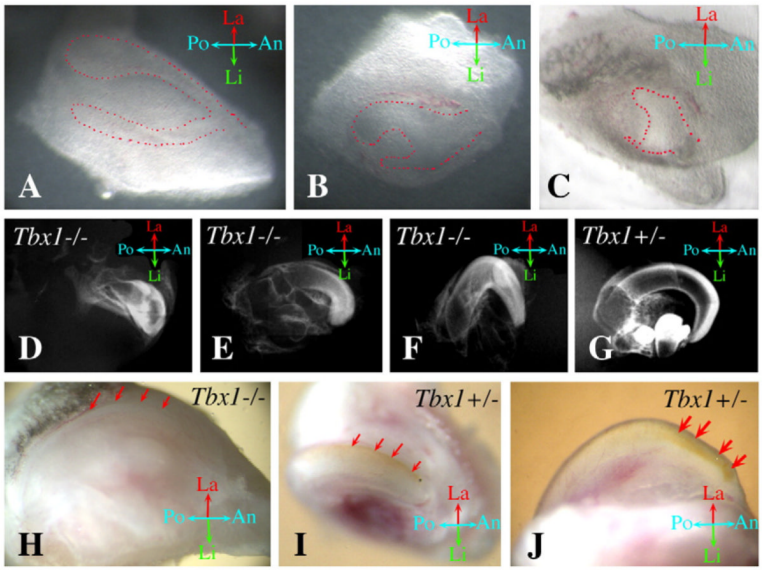

Fig. 4.

Transplantation and culture of incisor germs in kidney capsules. (A–C) Isolated incisor germs used for the culture in kidney capsules. Dotted red lines outline the epithelial part of the incisors. (D–G) X-rays of *Tbx1*−/− (D–F) and *Tbx1*+/− (G) incisors developed in kidney capsules for 28 days. (H–J) Macroscopic vu of incisors grown in kidney capsules for 28 days. Red arrows indicate the side where the enamel is normally formed (yellow color). No yellow color is seen in the *Tbx1*−/− (H) incisors, while in the *Tbx1*+/− incisors (I, J) the color is evident. Abbreviations: An, anterior part; La, labial side; Li, lingual side; Po, posterior part.

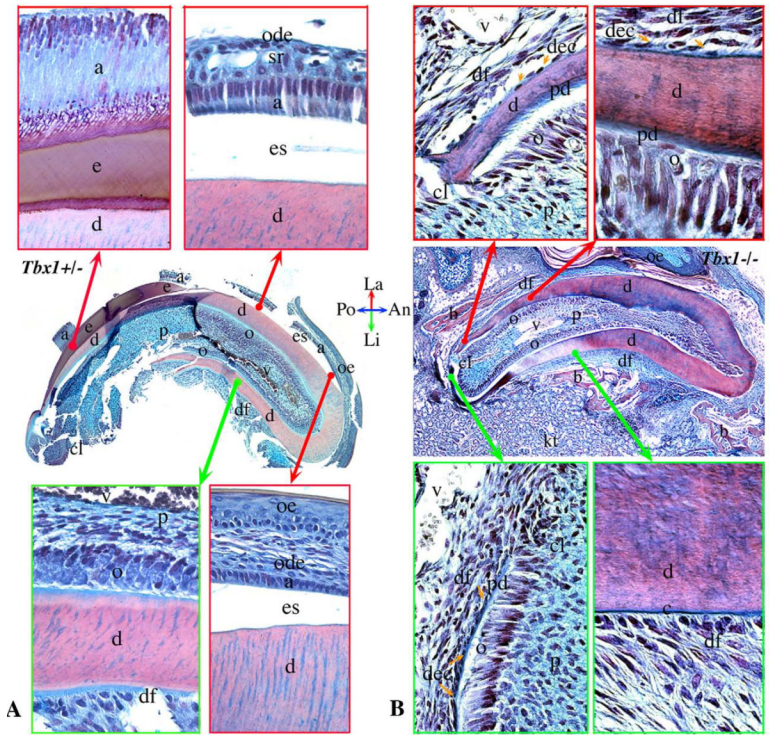

Fig. 5.

Histological examination of incisors developed in kidney capsules. Histological preparations of *Tbx1*+/− (A; left side) and *Tbx1*−/− (B; right side) incisors grown for 28 days. Red color boxes represent high magnifications of the labial side where normally enamel forms. Green color boxes are high magnifications of the areas in the lingual side. (A) Ameloblasts (a) and enamel (e) is detected in the *Tbx1*+/− incisors. (B) Ameloblasts and enamel are absent in the *Tbx1*−/− incisors. Orange arrows indicate cementoblasts. Additional abbreviations: An, anterior part; b, bone; c, cementum; cl, cervical loop; d, dentin; dec, dental cementoblasts; df, dental follicle; es, enamel space; kt, kidney tissue; La, labial side; Li, lingual side; o, odontoblast; ode, outer dental epithelium; oe, oral epithelium; p, pulp; pd, predentin; Po, posterior part; sr, stellate reticulum; v, vessels.

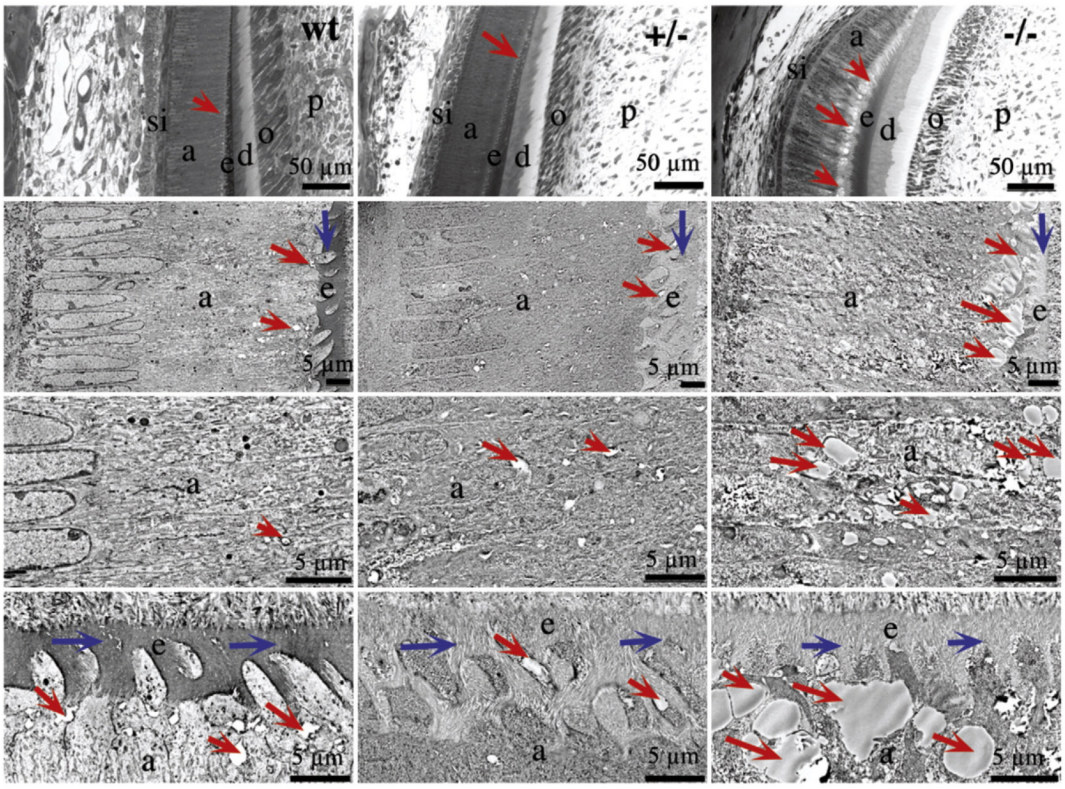

Fig. 6.

Structural alterations in the ameloblasts of *Tbx1*−/− incisors developed in kidney capsules. Light- (top row) and transmission electron micrographs (rows 2–4) of the forming enamel and ameloblasts of wild-type (left column), *Tbx1*+/− (middle column), and *Tbx1*−/− (right column) incisors grown in kidney capsules for 28 days. Red arrows point to vacuoles in the cytoplasm and at the secreting pole of ameloblasts. Blue arrows point to the enamel formation front. Abbreviations: a, ameloblasts; d, dentin; e, enamel; o, odontoblasts; p, pulp; si, stratum intermedium; wt, wild-type.

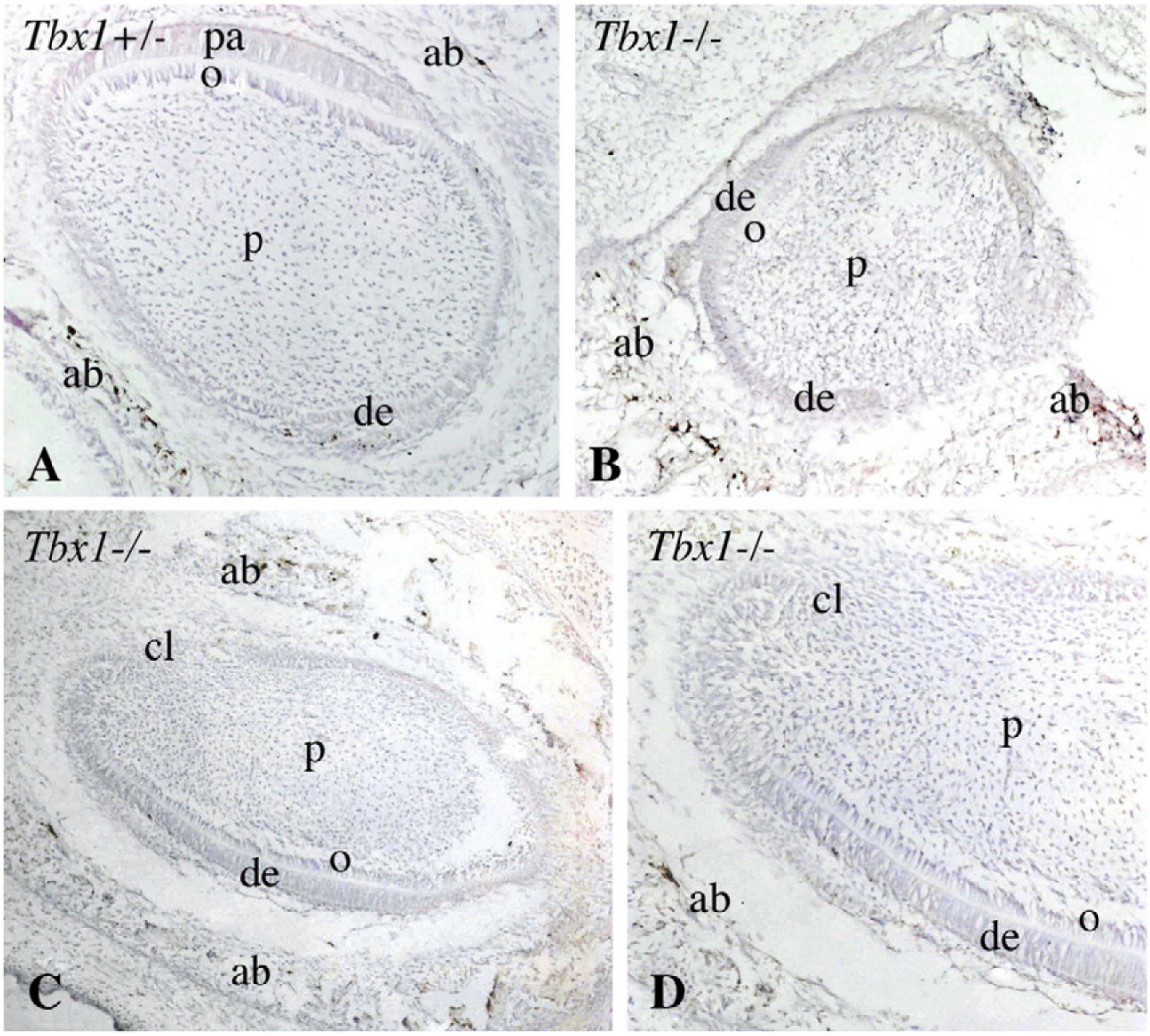

Fig. 7.

Cell apoptosis in *Tbx1*−/− incisors. Frontal (A, B) and longitudinal sections (C, D). *Tbx1*+/− (A) and *Tbx1*−/− (B–D) E18.5 incisors. Apoptotic cells exhibit a brown color. (A) Very few apoptotic epithelial cells are detected in the *Tbx1*+/− maxillary incisor. Apoptosis is evident in cells of the alveolar bone (ab). (B, D) Apoptosis is not detected in epithelial cells of the maxillary (B) and mandibular (C) incisors. Note apoptosis in the alveolar bone. (D) Higher magnification of the previous figure focusing in the cervical loop and transition areas of the mandibular incisor. Abbreviations: cl, cervical loop; de, dental epithelium; o, odontoblasts; p, dental pulp; pa, preameloblasts.

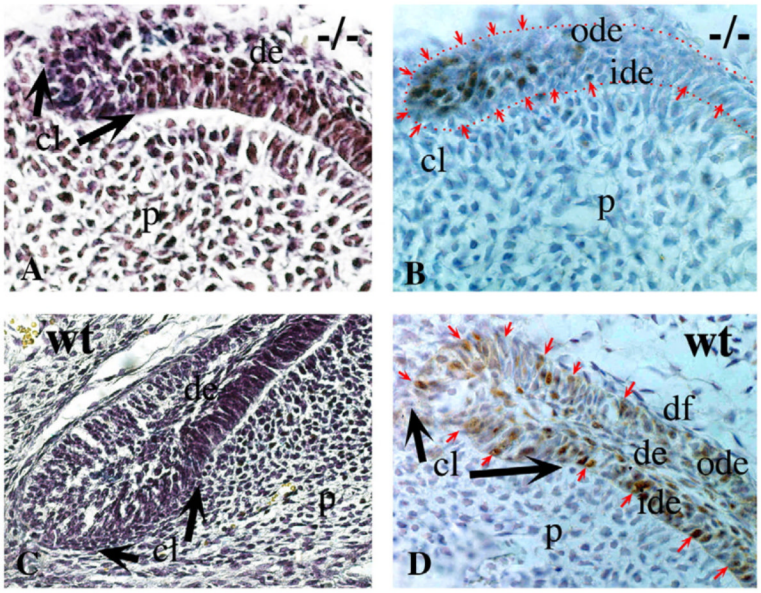

Fig. 8.

Altered epithelial cell proliferation in *Tbx1*−/− incisors. High magnifications of the cervical loop area on the labial side of *Tbx1*−/− (A, B) and wild-type (C, D) E18.5 incisors. Proliferating cells exhibit a brown color after PCNA immunostaining. (A) Histology of the cervical loop of a mutant incisor. (B) Proliferating epithelial cells are restricted in the cervical loop area of a mutant incisor. Red dots indicate the form of dental epithelium. Red arrows indicate cells of the inner and outer dental epithelium. Note that proliferation is seen in epithelial cells of the inner cell mass. No proliferation is seen in inner dental epithelium. (C) Histology of the cervical loop of a wild-type incisor. (D) Intense cell proliferation is detected in all epithelial cell layers of a wild-type incisor. Red arrows indicate cells of the inner and outer dental epithelium. Note massive cell proliferations in cells of the inner dental epithelium. Abbreviations: cl, cervical loop; de, dental epithelium; df, dental follicle; ide, inner dental epithelium; p, dental pulp; wt, wild-type.

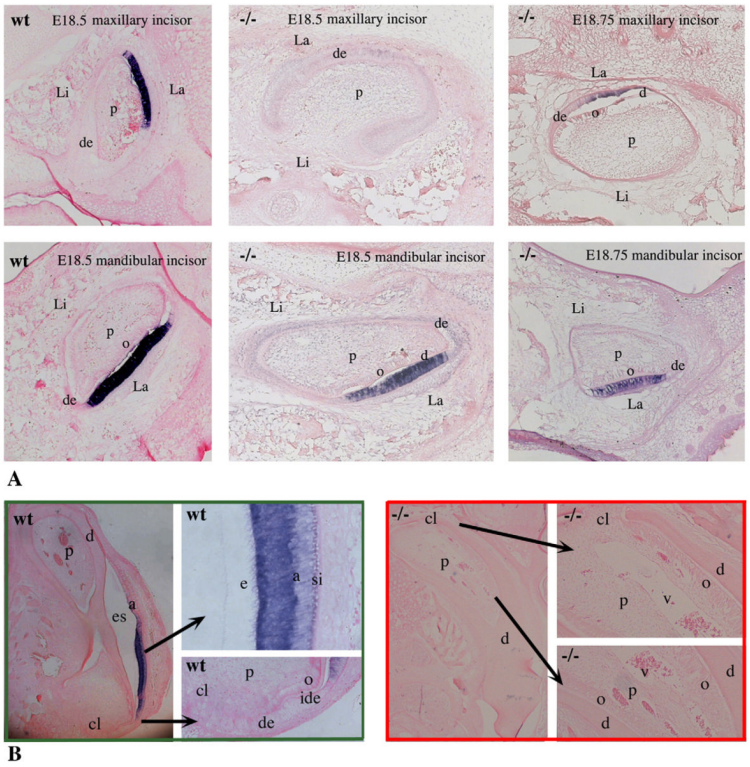

Fig. 9.

Patterns of *amelogenin* expression in developing and mature wild-type and *Tbx1*−/− incisors. In situ hybridization on paraffin sections. (A) Expression of *amelogenin* in maxillary and mandibular E18.5–E18.75 wild-type (wt) and *Tbx1*−/− mouse incisors. Note that expression is stronger in wild-type incisors than in mutant incisors. The hybridization signal is stronger in the mandibular mutant incisors when compared to that of the maxillary incisors. (B) Expression of *amelogenin* on *Tbx1*−/− (red box) and wild-type (red box) incisors cultured in kidney capsules for 28 days. *Amelogenin* expression is absent in the *Tbx1*−/− incisors. Abbreviations: a, ameloblasts; cl, cervical loop; d, dentin; de, dental epithelium; e, enamel; es, enamel space; ide, inner dental epithelium; La, labial side; Li, lingual side; o, odontoblasts; p, dental pulp; si, stratum intermedium; v, vessels.

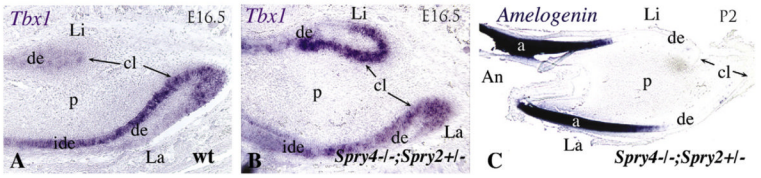

Fig. 10.

Patterns of *Tbx1* and *amelogenin* expression in developing wild-type and *Spry4−/−;Spry2+/−* incisors. In situ hybridization on cryosections. (A) Expression of *Tbx1* in an E16.5 wild-type incisor. (B) Expression of *Tbx1* in an E16.5 *Spry4−/−;Spry2+/−* incisor. Note that *Tbx1* is expressed in the lingual side and the labial side. (C) *Amelogenin* expression in a P2 *Spry4−/−;Spry2+/−* incisor. Note that amelogenin is expressed in both lingual and labial sides. Abbreviations: a, ameloblasts; An, anterior part; cl, cervical loop; d, dentin; de, dental epithelium; ide, inner dental epithelium; La, labial side; Li, lingual side; o, odontoblasts; p, dental pulp; wt, wild-type.

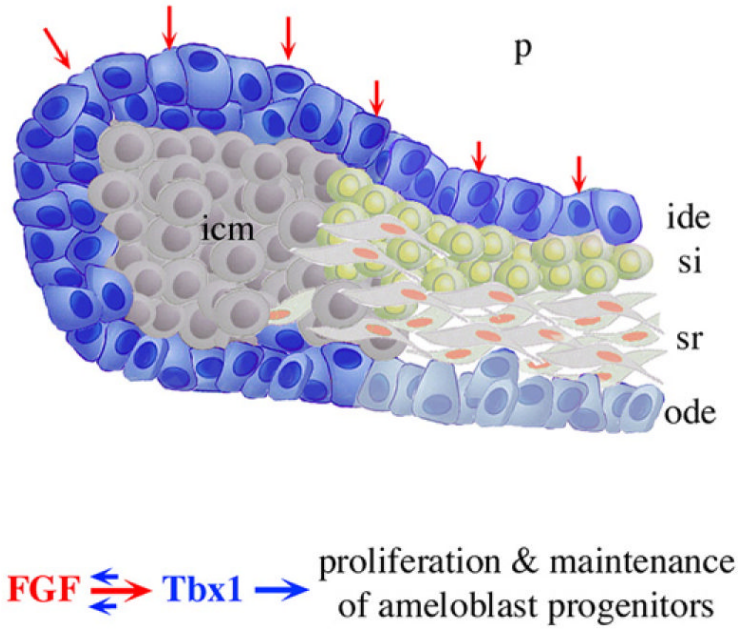

Fig. 11.

Schematic representation of a model illustrating the effects of Tbx1 in the proliferation and maintenance of the ameloblast progenitors. Cells of the stem cell niche at the cervical loop of the rodent incisor that express Tbx1 (dark blue cells of the inner dental epithelium) will give rise to ameloblasts and form enamel. Tbx1 forms a regulatory loop with FGFs in teeth. Tbx1, in combination with FGF molecules (red arrows), promotes the proliferation and maintenance of ameloblast progenitors in incisors. Proliferation of cells of the inner dental epithelium (i.e. ameloblast progenitors), but not of cells of the inner cell mass (icm), is disrupted after Tbx1 deletion. As a consequence of this disruption ameloblast differentiation and enamel matrix production are severely affected. Additional abbreviations: ide, inner dental epithelium; ode, outer dental epithelium; p, dental pulp; si, stratum intermedium; sr, stellate reticulum.